Supporting Information for

Stable seawater oxidation with a self-healing oxygen-evolving catalyst

Xiaojian Zhang,[a,b] Chao Feng,[b] Zeyu Fan,[b] Beibei Zhang,[b] Yequan Xiao,[c] Andraž Mavrič,[d] Nadiia Pastukhova,[d] Matjaz Valant,[d] Yi-Fan Han,*[a] and Yanbo Li*[b]

[a]Engineering Research Center of Advanced Functional Material Manufacturing of Ministry of Education, Zhengzhou University, Zhengzhou 450001, China. *Email: yifanhan@ecust.edu.cn

[b]Institute of Fundamental and Frontier Sciences, University of Electronic Science and Technology of China, Chengdu 610054, China. *Email: yanboli@uestc.edu.cn

[c]School of Physics and Optoelectronics, Xiangtan University, Xiangtan 411105, China.

[d]University of Nova Gorica, Materials Research Laboratory, Vipavska 13, SI-5000 Nova Gorica, Slovenia.

Materials and Methods

Chemicals. Fe (II) sulfate heptahydrate ($FeSO_4 \cdot 7H_2O$, 99.95%; Aladdin); Co (II) nitrate hexahydrate ($Co(NO_3)_2 \cdot 6H_2O$, 99.99%; Aladdin); Ni (II) nitrate hexahydrate ($NiSO_4 \cdot 6H_2O$, 99.99%; Aladdin); Hydrochloric acid (HCl, 37%; RCI Labscan Limited), potassium hydroxide (KOH, 95%; Aladdin), boric acid (H_3BO_3, 99.5%; Aladdin), Ni foam (thickness, 2 mm), and Argon (Ar, 99.999%) were used as received. Deionized (DI) water was used for the preparation of all aqueous solutions. The artificial seawater was prepared according to the Standard Practice for Preparation of Substitute Ocean Water (ASTM D1141-98). Natural seawater (pH∼7.3) was collected from the silver beach in Lushan, Weihai, Shandong, China (36.494° N, 121.424° E).

Synthesis of NiCoFe-B_i and NiCo-B_i catalysts on NF. The NiCoFe-B_i catalyst was deposited on the NF substrate via an electrodeposition process. Before the synthesis, NF substrates (0.5 cm^{-2}) were sequentially cleaned with 6 M hydrochloric acid, deionized water, acetone, and anhydrous ethanol by ultrasonication for 15 min each to remove the possible surface oxide layer and ensure the clean surface, then dried under a flow of nitrogen gas. Next, the NiCoFe-B_i catalyst was electrodeposited onto NF substrates in potassium borate buffer (pH 10) containing Ni(II), Co(II), and Fe(II) ions. Potassium borate ($K_2B_4O_5(OH)_4$, KB_i) buffer was prepared by mixing 1 M boric acid with 0.6 M potassium hydroxide. Prior to electrodeposition, the buffer solution is continuously fed with Ar gas to remove the oxygen for at least 10 minutes. Then, 0.5 mM cobalt(II) nitrate, 2 mM nickel(II) sulfate, and 0.8 mM iron(II) sulfate were sequentially added to the KB_i buffer solution under magnetic stirring. The solution was under continuous Ar bubbling and magnetic stirring during electrodeposition. Electrodeposition was conducted with a potentiostat (BioLogic SP-200) in

a three-electrode configuration using Ag/AgCl as the reference electrode and a Pt wire as the counter electrode. The NiCoFe-B_i catalyst was deposited on NF substrate under a constant voltage of 0.85V for 30 min. After electrodeposition, the electrode was washed thoroughly with deionized water before the OER test. NiCo-B_i catalyst was deposited onto NF substrates in a similar way to that used for NiCoFe-B_i deposition except that Fe(II) ions were not added.

Preparation of artificial seawater. Firstly, 396.858 g $MgCl_2{\cdot}6H_2O$, 41.815 g $CaCl_2$ and 1.484 g $SrCl_2{\cdot}6H_2O$ were dissolved in DI water and diluted to a total volume of 700 mL. The solution was stored in well stoppered glass containers as the Stock Solution No. 1.

Then, 48.671 g KCl, 14.140 g $NaHCO_3$, 7.112 g KBr, 1.911 g H_3BO_3, and 0.217 g NaF were dissolved in DI water and diluted to a total volume of 700 mL. The solution was stored in well stoppered glass containers as the Stock Solution No. 2.

To prepare 1.0 L of artificial seawater, 24.5586 g NaCl and 4.1354 g Na_2SO_4 were dissolved in 800 mL of DI water. Then 20 mL of Stock Solution No.1 and 10 mL of Stock Solution No.2 were sequentially added to the above 800 mL of mixed solution under magnetic stirring. Finally, the artificial seawater (pH~7.65) was obtained by diluting the above solution into 1L.

Alkaline treatment of artificial and natural seawater. The alkaline treatment of seawater at pH 14.95 was achieved by adding 10 M KOH into the seawater. To thoroughly remove $Mg^{2+}$and Ca^{2+}, the 10 M KOH was added sequentially into 1 L artificial seawater in three batches. After each addition, the solution was stirred continuously for 1h under magnetic stirring and then left to stand for 24 h to obtain a supernatant, which was then filtered using with a 5-μm capsule filter. Finally, to compensate for the possible loss of intercalated borate ions in the NiCoFe-B_i catalyst, 1 M H_3BO_3 was added into the solution to form 0.25 M $K_2B_4O_5(OH)_4$ (KB_i) in the seawater. The alkaline treatment of seawater at pH 14 and pH 14.6 were prepared in a similar way, except that 2 M and 5 M KOH were used, respectively.

Materials Characterization. The SEM and EDS of the catalysts were characterized using Phenom Pharos G2. A cross-sectional sample was prepared by mechanical polishing and finalized using ion beam polisher (JEOL IB-09010CP). The cross-sectional STEM-EDS mapping and line scan were obtained using JEOL JSM 7001 TTLS (FEG) equipped with an EDS detector (Oxford Instruments). After alkaline treatment at pH 14.95, the precipitates were characterized by X-Ray Diffraction (XRD, Thermo Scientific ARL^{TM} EQUINOX 1000) with Cu-Kα radiation, and the remaining concentrations of Mg^{2+} and Ca^{2+} in seawater were determined using ICP-optical emission spectrometry (ICP-OES; iCAP 7400DUO, Thermo Fisher Scientific). The surface chemical composition and valence states of the as-prepared and post-OER electrodes were analyzed by X-ray

photoelectron spectroscopy (XPS, Specs PHOIBOS 150) using Al-Kα radiation. The binding energy was calibrated by setting the binding energy of the hydrocarbon C 1s feature to 284.8 eV. Spectrum analysis was performed with the XPSPEAK software and the Thermo Scientific™ Avantage software.

Electrochemical Characterizations. The electrochemical tests were performed on a potentiostat (CHI 660E, CH Instruments, Inc.) in an H-cell in a three-electrode configuration. A Pt wire and a double-salt-bridge Hg/HgO electrode were used as the counter and reference electrodes, respectively. The anode chamber and the cathode chamber of the H-cell were separated using an anion exchange membrane (Sustainion X37-50, 4.9 cm^2). The H-cell was integrated with a water jacket and the temperature of the electrolyte was maintained at 25 °C using a constant temperature water circulator. OER polarization curves of the catalysts were measured under an anodic scan at a rate of 10 mV s^{-1} under magnetic stirring. The stability of the catalysts was tested under current densities of 100 or 500 mA cm^{-2}. The potentials vs. Hg/HgO reference electrodes were converted into RHE following the Nernst equation ($E_{RHE} = E_{Hg/HgO} + 0.0591 \times pH + 0.098$). The ohmic resistance (R_s) for iR corrections was determined by electrochemical impedance spectroscopy (EIS). EIS was conducted at an overpotential of 300 mV from 0.01 Hz to 10000 Hz with an AC amplitude of 10 mV. The Tafel slope curves were plotted from the corresponding LSV curves with iR compensation. To calculate FE, we measured the generated gaseous product in the flow cell configuration. An air-tight electrochemical cell with a gas inlet and outlet was used for the GC (Shimadzu GC-2014) measurement. The FE was calculated by comparing the experimentally measured O_2 amount to the theoretically calculated value from the current. By plotting the capacitive current at 1.08 V vs. RHE against the scan rates, the double-layer capacitance (C_{dl}) was obtained and then the ECSA was derived from the equation: ECSA = C_{dl}/C_s, in which C_s is the specific capacitance for a flat surface (40 μF cm^{-2}).

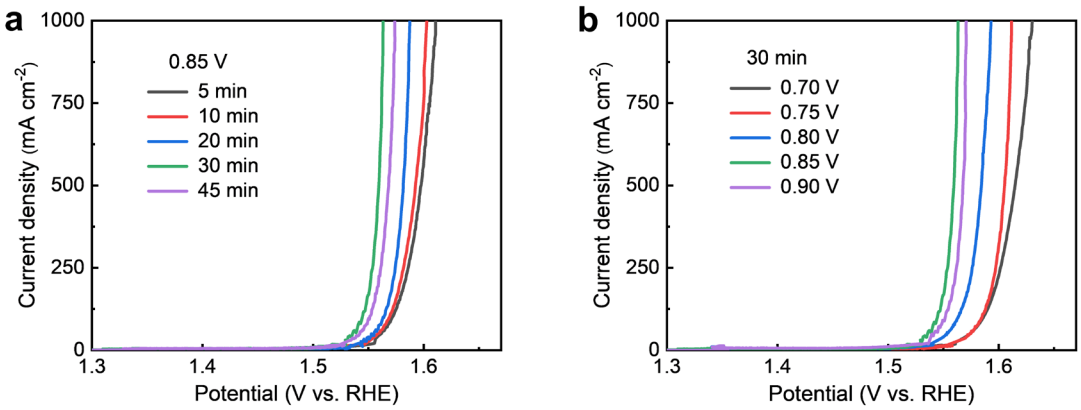

Fig. S1. The OER polarization curves of NiCoFe-B_i catalysts: (a) deposited at 0.85 V vs. Ag/AgCl for different electrodeposition times; (b) deposited at different applied potentials for 30 min. The curves were measured in alkaline artificial seawater (pH 14) with 0.05 mM Fe(II) ions at 10 mV s^{-1} scan rate, with iR correction.

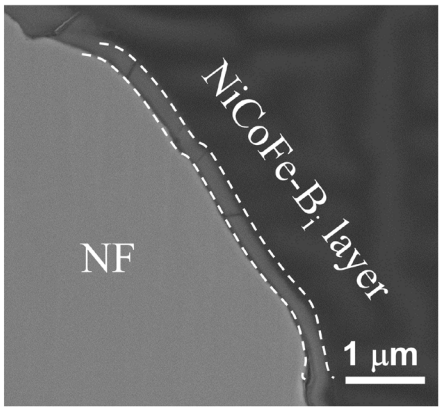

Fig. S2. The cross-sectional SEM image of NiCoFe-B_i catalyst on NF substrate.

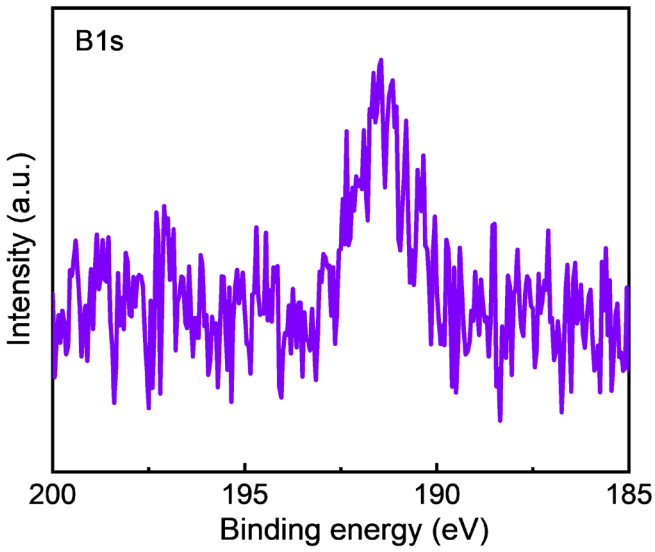

Fig. S3. Core-level XPS spectra of B 1*s* of the as-prepared NiCoFe-B_i catalyst.

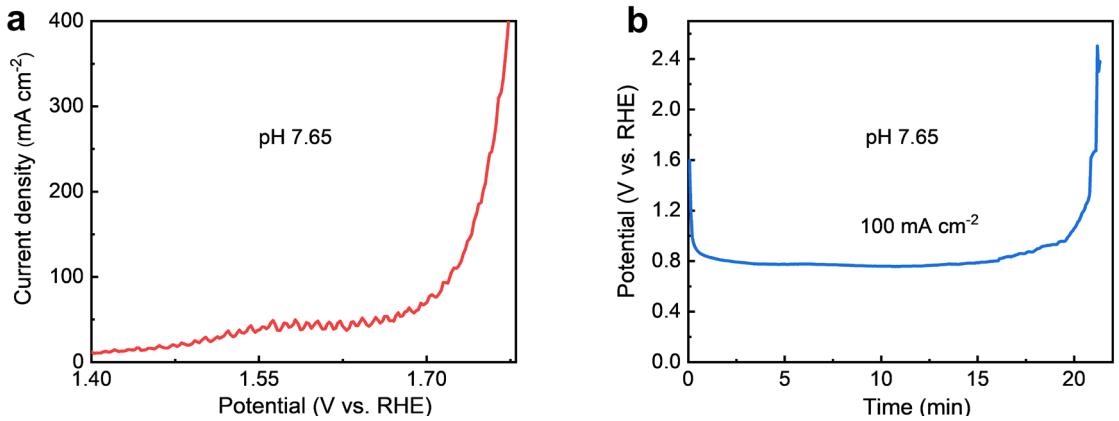

Fig. S4. OER performance of NiCoFe-B_i catalyst in artificial seawater at pH 7.65. (a) The LSV curve measured at 10 mV s^{-1} scan rate, without iR correction. (b) Chronoamperometry curve measured at 100 mA cm^{-2} for 20 min. Most likely the current is mainly derived from the electrochemical oxidation of the NF substrate until failure at 20 minutes.

Fig. S5. Photographs of NiCoFe-B_i/NF electrode: (a) as-prepared; (b, c) after stability test at 100 mA cm^{-2} for 20 min in artificial seawater at pH 7.65.

The electrode corrodes rapidly in untreated seawater likely due to the aggressive chloride anions in seawater, which corrode the catalyst and substrate through a metal chloride-hydroxide formation mechanism[1,2] (M represents metal atoms):

Adsorption of Cl^- by surface polarization: $M + Cl^- \rightarrow MCl_{ads} + e^-$

Dissolution by further coordination: $MCl_{ads} + Cl^- \rightarrow MCl_x^-$

Conversion from chloride to hydroxide: $MCl_x^- + OH^- \rightarrow M(OH)_x + Cl^-$

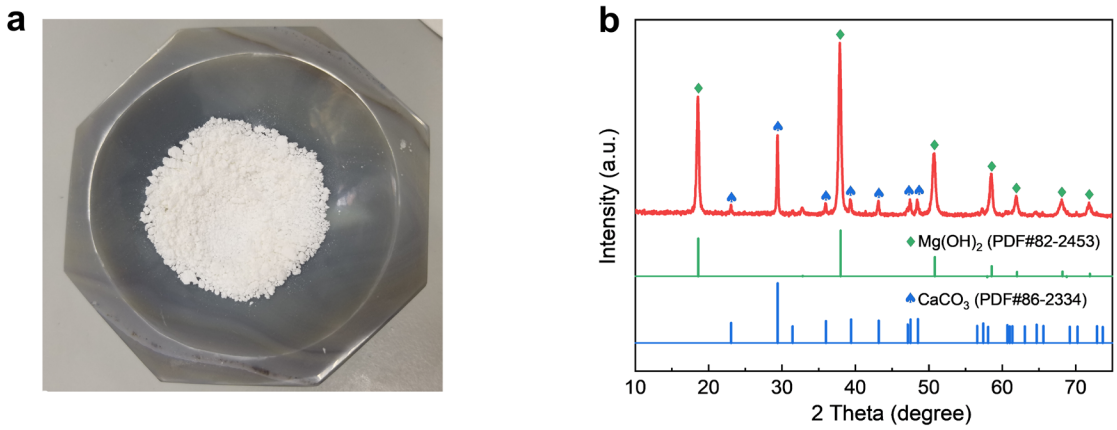

Fig. S6. (a) Photograph and (b) XRD pattern of the precipitates obtained by the alkaline treatment of artificial seawater at pH 14.95. The reference patterns of $Mg(OH)_2$ and $CaCO_3$ are shown for comparison.

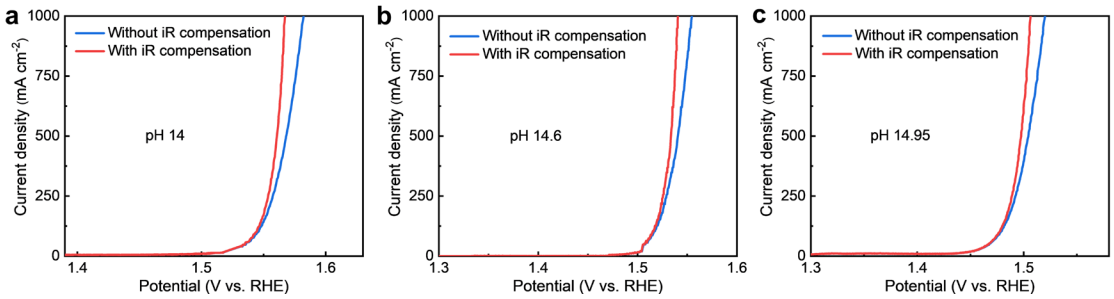

Fig. S7. The OER polarization curves of NiCoFe-B_i catalyst with and without iR correction in alkaline artificial seawater with Fe(II) ions at pH 14, 14.6, and 14.95, respectively.

Fig. S8. Photographs of NiCoFe-B_i/NF electrode: (a) as-prepared; (b, c) after stability test at 500 mA cm^{-2} for 15 h in artificial seawater at pH 14 with 0.05 mM Fe(II) ions.

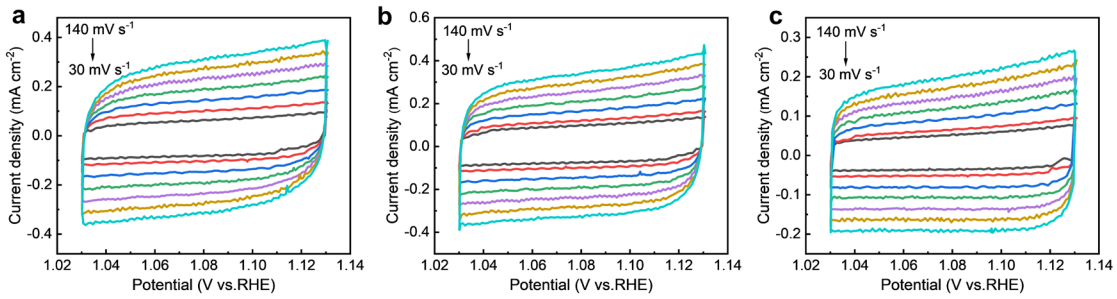

Fig. S9. The cyclic voltammetry (CV) curves measured at different scan rates in the potential range of the non-Faraday region (1.02 V ~ 1.14 V vs. RHE). (a) The as-deposited NiCoFe-B_i catalyst in artificial seawater at pH 14.95 with 0.5 mM Fe(II) ions. (b) After OER test at 500 mA cm^{-2} for 100 h in artificial seawater at pH 14.95 with 0.5 mM Fe(II) ions. (c) NiCoFe-B_i catalyst in artificial seawater at pH 14.95 without the addition of Fe(II) ions.

Calculation of ECSA for the NiCoFe-B_i catalyst:

$ECSA = C_{dl}/C_s$

With the addition of 0.5 mM Fe(II) ions:

ECSA = 4.33 mF cm^{-2}/40 μF cm^{-2} = 108.25 cm^{-2} (as-deposied)

ECSA = 4.53 mF cm^{-2}/40 μF cm^{-2} = 113.25 cm^{-2} (post-OER)

Without the addition of Fe(II) ions:

ECSA = 2.81 mF cm^{-2}/40 μF cm^{-2} = 70.25 cm^{-2}

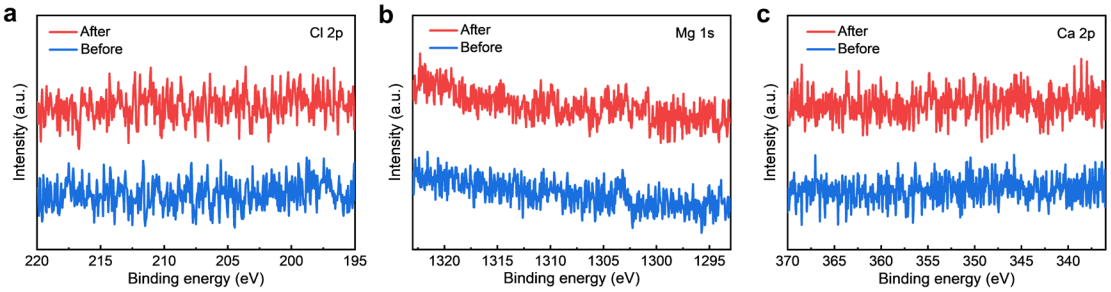

Fig. S10. Core-level XPS spectra of the NiCoFe-B_i catalyst before and after the stability test at 500 mA cm^{-2} for 100 h in artificial seawater at pH 14.95 with 0.5 mM Fe(II) ions: (a) Cl 2*p*, (b) Mg 1*s*, and (c) Ca 2*p*.

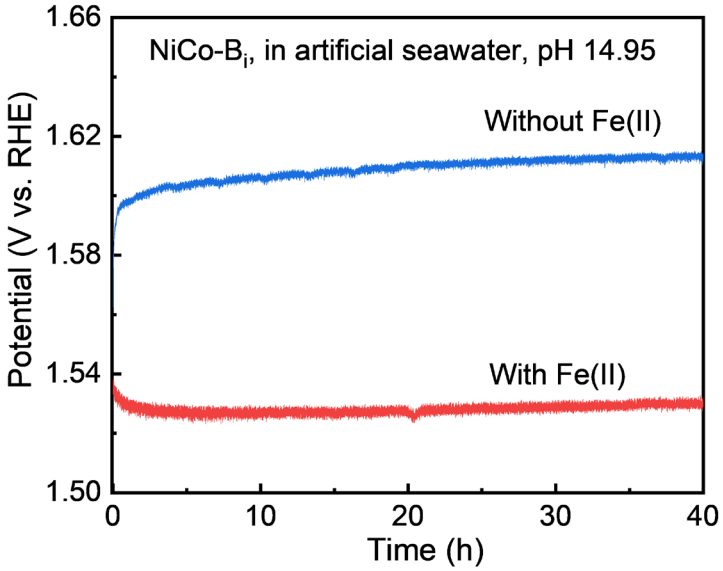

Fig. S11. Chronopotentiometry curves of NiCo-B_i catalyst measured at 500 mA cm^{-2} for 40 h in artificial seawater at pH 14.95 with and without the addition of Fe(II) ions.

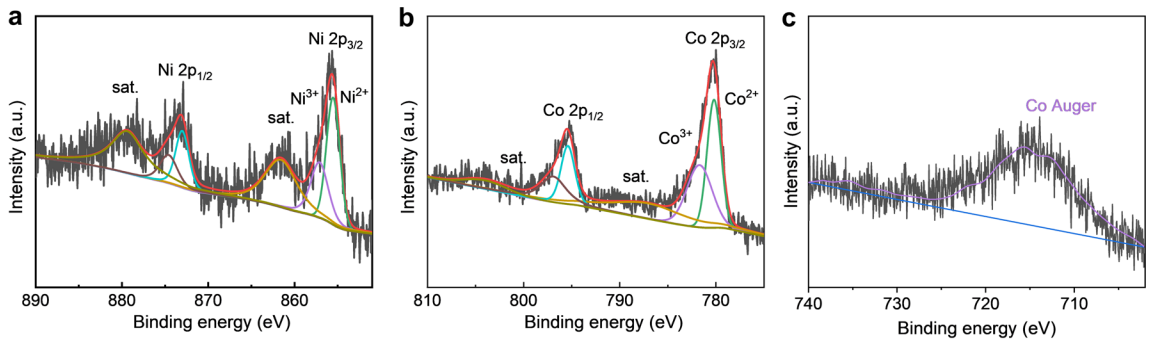

Fig. S12. Core-level XPS spectra of the NiCoFe-B_i catalyst after the stability test at 500 mA cm^{-2} for 60 h in artificial seawater at pH 14.95 without Fe(II) ions: (a) Ni 2*p*, (b) Co 2*p*, and (c) Fe 2*p*. It should be noted that the peak in the Fe 2p region can be well-fitted using only the Co Auger reference spectrum (purple line) by the NLLSF function, suggesting there is almost no Fe 2p signal.

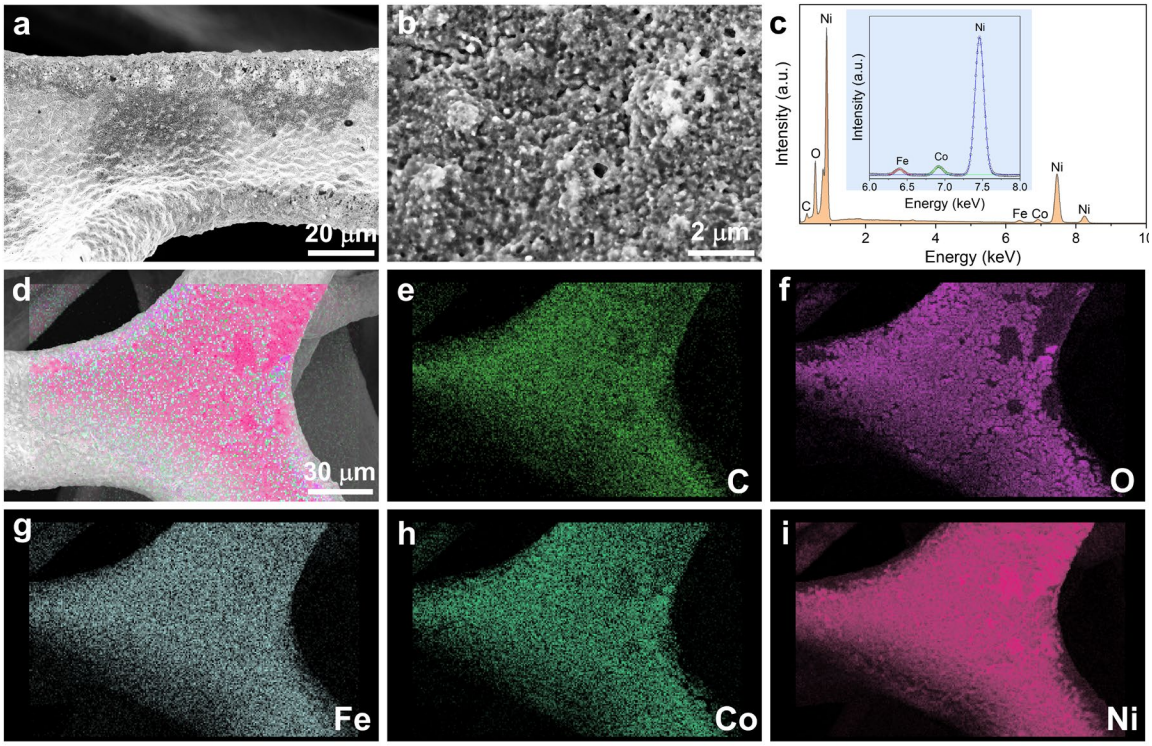

Fig. S13. Morphological and compositional characterizations of the NiCoFe-B_i catalyst after stability test at 500 mA cm^{-2} for 100 h in artificial seawater at pH 14.95 with 0.5 mM Fe(II) ions. (a, b) SEM images at different magnifications. (c) EDS spectrum, inset shows the Lα lines of Ni, Co, and Fe. (d-i) SEM image of a NiCoFe-B_i layer on NF substrate and the corresponding EDS mappings of C, O, Fe, Co, and Ni elements.

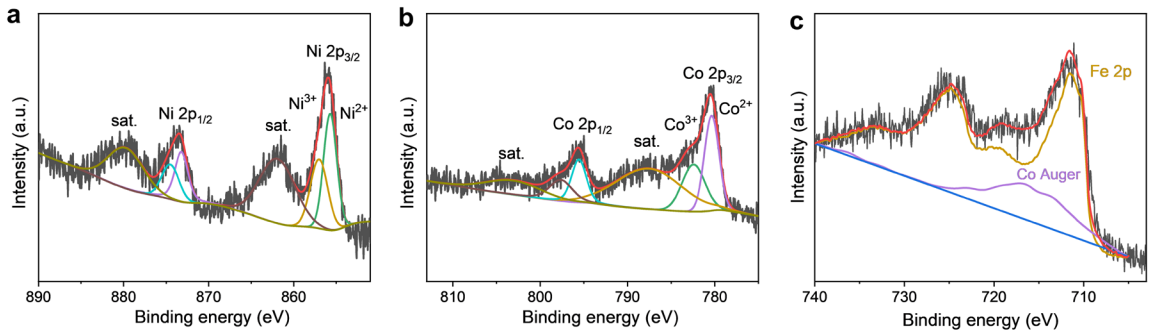

Fig. S14. Core-level XPS spectra of the NiCoFe-B_i catalyst after the stability test at 500 mA cm^{-2} for 100 h in artificial seawater at pH 14.95 with 0.5 mM Fe(II) ions: (a) Ni 2*p*, (b) Co 2*p*, and (c) Fe 2*p*.

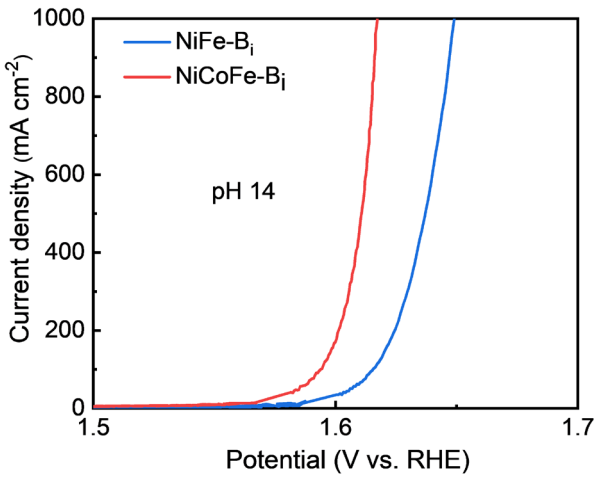

Fig. S15. LSV curves of NiFe-B_i and NiCoFe-B_i catalysts in artificial seawater at pH 14 with 0.05 mM Fe(II) ions. The OER polarization curves were measured at 10 mV s^{-1} scan rate, without iR correction.

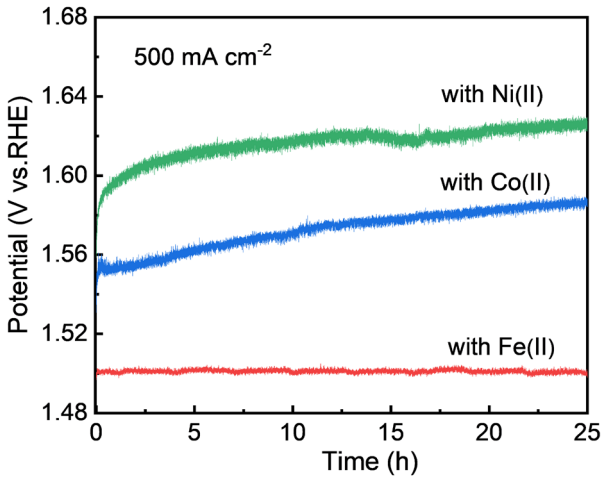

Fig. S16. Chronopotentiometry curves of NiCoFe-B_i catalyst measured at 500 mA cm^{-2} in artificial seawater (pH 14.95) with the addition of Fe(II), Co(II), or Ni(II) ions.

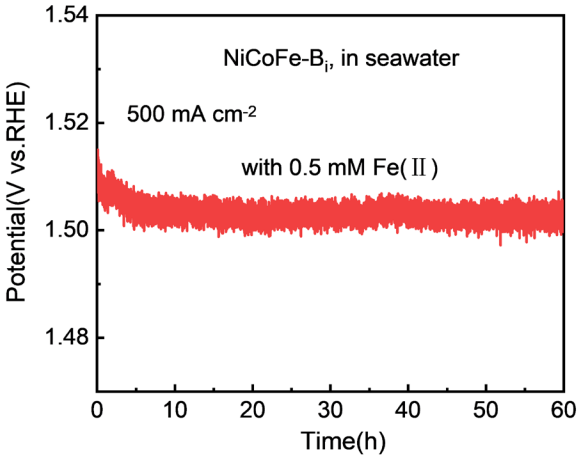

Fig. S17. Chronopotentiometry curve of NiCoFe-B_i catalyst measured at 500 mA cm^{-2} for 60 h in artificial seawater at pH 14.95 without adding additional borate ions.

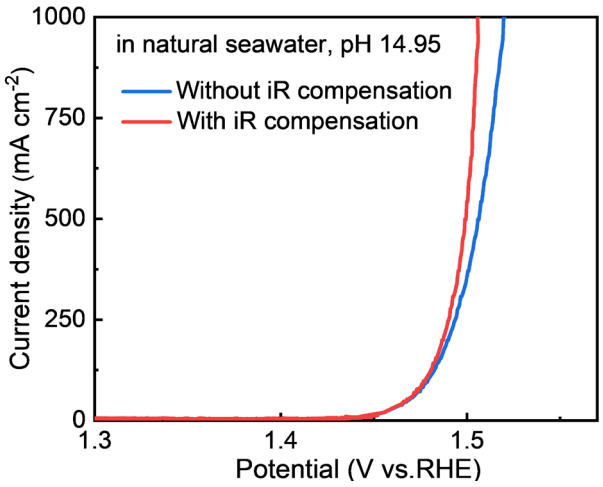

Fig. S18. The OER polarization curves of the NiCoFe-B_i catalyst in natural seawater at pH 14.95 with 0.5 mM Fe(II) ions. The curves were measured at 10 mV s^{-1} scan rate with and without iR correction.

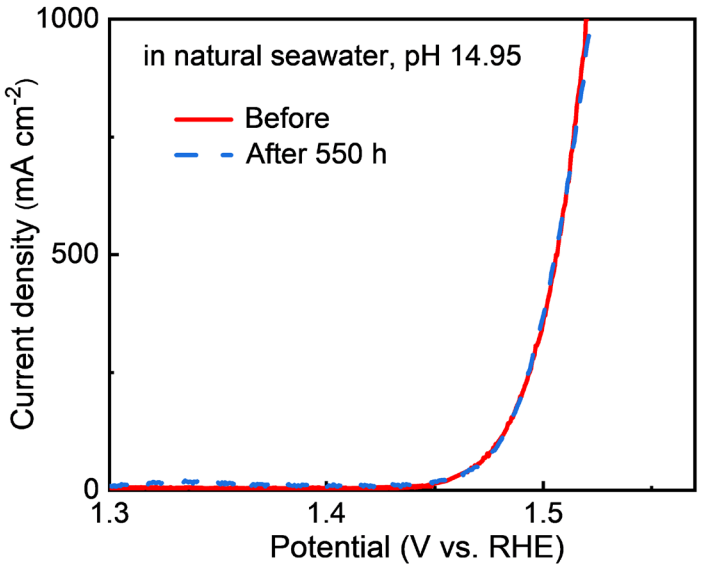

Fig. S19. The OER polarization curves of the NiCoFe-B_i catalyst before and after 550 h stability test at 500 mA cm^{-2} in natural seawater at pH 14.95 with 0.5 mM Fe(II) ions. The curves were measured at 10 mV s^{-1} scan rate, without iR correction.

Table S1. Chemical composition of artificial seawater prepared according to the Standard Practice for Preparation of Substitute Ocean Water (ASTM D1141-98)

Compound	Concentration, g/L
NaCl	24.5586
$MgCl_2 \cdot 6H_2O$	11.3388
$CaCl_2$	1.1947
Na_2SO_4	4.1354
KCl	0.6953
$NaHCO_3$	0.2020
KBr	0.1016
H_3BO_3	0.0273
$SrCl_2 \cdot 6H_2O$	0.0424
NaF	0.0031

Table S2. Quantitative XPS analysis results of the atomic concentrations of Fe, Co, and Ni elements in the as-deposited NiCoFe-B_i catalyst and after the OER test in artificial seawater (pH 14.95, with 0.5 mM Fe(II) ions) at 500 mA cm^{-2} for 100 h.

	Element	Line	Area	ASF	Area/ASF	Atomic conc. (%)
As-deposited	Fe	2p	12488.8	2.957	4223.5	34.4
	Co	2p	17114.9	3.590	4767.4	38.9
	Ni	2p	13246.4	4.044	3275.6	26.7
After OER test	Fe	2p	16719.9	2.957	5654.3	44.3
	Co	2p	13443.5	3.590	3744.7	29.3
	Ni	2p	13603.9	4.044	3364.0	26.4

Table S3. The concentration of Mg and Ca elements (ppm) in artificial seawater before and after alkaline treatment at pH 14.95.

	Mg	Ca
Untreated	1314	417.6
Alkaline treatment	0.43	6.16

The concentration of Mg and Ca elements (ppm) of untreated artificial seawater was calculated from the amount of $MgCl_2$ and $CaCl_2$ used to prepare the artificial seawater according to ASTM D1141-98 (Table S1), while the values after alkaline treatment at pH 14.95 were obtained by ICP-OES analysis.

Table S4. Fitted parameters of the EIS Nyquist plots of NiCoFe-B_i/NF electrodes tested in different electrolyte conditions.

Electrolyte conditions	R_s (Ω)	R_{ct} (Ω)	C_{dl} (F)
Artificial seawater, pH 14.95, with 0.5 mM Fe(II)	0.0285	0.196	0.0643
Artificial seawater, pH 14.95, without Fe(II)	0.0286	2.013	0.0366
Natural seawater, pH 14.95, with 0.5 mM Fe(II)	0.0251	0.213	0.1162

Table S5. Comparison of the stability of NiCoFe-B_i catalyst with recently reported OER catalysts for seawater electrolysis.

Catalyst	Electrolyte	J (mA cm^{-2})	Testing time (h)	Δη (mV)	Ref.
NiCoFe-B_i/NF	Artificial seawater (pH14.95)	500	1000	Negligible	This work
	Natural seawater (pH 14.95)	500	550	Negligible	
Fe-NiSOH	1 M KOH + natural seawater	500	900	49	3
NiFe-CuCo LDH	1 M KOH + 1.5 M NaCl	500	50	34	4
	6 M KOH + natural seawater	500	500	71	
Gd-Mn_3O_4@CuO-$Cu(OH)_2$	1 M KOH + natural seawater	100	75	45	5
V-doped CoCr LDH	1 M KOH + natural seawater	20	24	NA	6
CoP_x@FeOOH	1 M KOH + natural seawater	100	80	29	7
		500	80	70	
Fe-$Ni(OH)_2$/Ni_3S_2/NF	1 M KOH + 0.5 M NaCl	100	27	~15	8
Cu@Co-CoO/Rh	1 M KOH + 0.5 NaCl	10	10	NA	9
Ni_3S_2/Co_3S_4	1 M KOH + natural seawater	100	10	NA	10
Ni_2P-Fe_2P/NF	1 M KOH + natural seawater	100	36	18	11
		500	24	52	
Ni-doped FeOOH/NF	1 M KOH + 0.5 M NaCl	100	80	~25	12
NiFe LDH/NiS	1 M KOH + 0.5 M NaCl	400	24	NA	13
NiFe LDH	1 M KOH + natural seawater	500	96	NA	14
NiFe/$NiFeB_x$	30 wt% KOH electrolyte + 0.5 M NaCl	100	125	NA	15
B-Co_2Fe LDH	1 M KOH + natural seawater	100	100	46	16
		500	100	65	
S-Ni/Fe(OOH)/NF	1 M KOH + natural seawater	100	100	NA	17
	1 M KOH + 1 M NaCl	100	100	NA	
GO@Fe@Ni-Co/NF	1 M KOH + 0.5 M NaCl	1000	12	~130	18
$Fe_{0.01}$-Ni&$Ni_{0.2}Mo_{0.8}N$	6 M KOH + natural seawater	1000	80	NA	19
NiCoFeP	6 M KOH + 2.8 M NaCl	500	100	NA	20

SI References

1. Y. Kuang, M. J. Kenney, Y. Meng, W. H. Hung, Y. Liu, J. E. Huang, R. Prasanna, P. Li, Y. Li, L. Wang, M. C. Lin, M. D. McGehee, X. Sun and H. Dai, Solar-driven, highly sustained splitting of seawater into hydrogen and oxygen fuels, *Proc. Natl. Acad. Sci. U. S. A.*, 2019, **116**, 6624-6629.
2. L. Yu, Q. Zhu, S. Song, B. McElhenny, D. Wang, C. Wu, Z. Qin, J. Bao, Y. Yu, S. Chen and Z. Ren, Non-noble metal-nitride based electrocatalysts for high-performance alkaline seawater electrolysis, *Nat. Commun.*, 2019, **10**, 5106.
3. C. Huang, Q. Zhou, D. Duan, L. Yu, W. Zhang, Z. Wang, J. Liu, B. Peng, P. An, J. Zhang, L. Li, J. Yu and Y. Yu, The rapid self-reconstruction of Fe-modified Ni hydroxysulfide for efficient and stable large-current-density water/seawater oxidation, *Energy Environ. Sci.*, 2022, **15**, 4647-4658.
4. L. Yu, J. Xiao, C. Huang, J. Zhou, M. Qiu, Y. Yu, Z. Ren, C. W. Chu and J. C. Yu, High-performance seawater oxidation by a homogeneous multimetallic layered double hydroxide electrocatalyst, *Proc. Natl. Acad. Sci. U. S. A.*, 2022, **119**, 2202382119.
5. T. Ul Haq, S. Mansour and Y. Haik, Electronic and structural modification of Mn_3O_4 nanosheets for selective and sustained seawater oxidation, *ACS Appl. Mater. Interfaces*, 2022, **14**, 20443-20454.
6. S. Khatun and P. Roy, Cobalt chromium vanadium layered triple hydroxides as an efficient oxygen electrocatalyst for alkaline seawater splitting, *Chem. Commun. (Camb)*, 2022, **58**, 1104-1107.
7. L. Wu, L. Yu, B. McElhenny, X. Xing, D. Luo, F. Zhang, J. Bao, S. Chen and Z. Ren, Rational design of core-shell-structured CoP_x@FeOOH for efficient seawater electrolysis, *Appl. Catal., B*, 2021, **294**, 120256.
8. B. Cui, Z. Hu, C. Liu, S. Liu, F. Chen, S. Hu, J. Zhang, W. Zhou, Y. Deng, Z. Qin, Z. Wu, Y. Chen, L. Cui and W. Hu, Heterogeneous lamellar-edged Fe-$Ni(OH)_2$/Ni_3S_2 nanoarray for efficient and stable seawater oxidation, *Nano Research*, 2020, **14**, 1149-1155.
9. P. K. L. Tran, D. T. Tran, D. Malhotra, S. Prabhakaran, D. H. Kim, N. H. Kim and J. H. Lee, Highly effective freshwater and seawater electrolysis enabled by atomic Rh-Modulated Co-CoO lateral heterostructures, *Small*, 2021, **17**, 2103826.
10. C. Wang, M. Zhu, Z. Cao, P. Zhu, Y. Cao, X. Xu, C. Xu and Z. Yin, Heterogeneous bimetallic sulfides based seawater electrolysis towards stable industrial-level large current density*, Appl. Catal.*, *B*, 2021, **291**, 120071.
11. L. Wu, L. Yu, F. Zhang, B. McElhenny, D. Luo, A. Karim, S. Chen and Z. Ren, Heterogeneous bimetallic phosphide Ni_2P-Fe_2P as an efficient bifunctional catalyst for water/seawater splitting, *Adv. Funct. Mater.*, 2020, **31**, 2006484.
12. Y. S. Park, J. Lee, M. J. Jang, J. Yang, J. Jeong, J. Park, Y. Kim, M. H. Seo, Z. Chen and S. M. Choi, High-performance anion exchange membrane alkaline seawater electrolysis, *J. Mater. Chem. A*, 2021, **9**, 9586-9592.
13. Q. Wen, K. Yang, D. Huang, G. Cheng, X. Ai, Y. Liu, J. Fang, H. Li, L. Yu and T. Zhai, Schottky heterojunction nanosheet array achieving high-current-censity oxygen evolution for industrial water splitting electrolyzers, *Adv. Energy Mater.*, 2021, **11**, 2102353.
14. M. Ning, L. Wu, F. Zhang, D. Wang, S. Song, T. Tong, J. Bao, S. Chen, L. Yu and Z. Ren, One-step spontaneous growth of NiFe layered double hydroxide at room temperature for seawater oxygen evolution, *Mater. Today Phys.*, 2021, **19**, 100419.
15. J. Li, Y. Liu, H. Chen, Z. Zhang and X. Zou, Design of a multilayered oxygen-evolution electrode with high catalytic activity and corrosion resistance for saline water splitting, *Adv. Funct. Mater.*, 2021, **31**, 2101820.
16. L. Wu, L. Yu, Q. Zhu, B. McElhenny, F. Zhang, C. Wu, X. Xing, J. Bao, S. Chen and Z. Ren, Boron-modified cobalt iron layered double hydroxides for high efficiency seawater oxidation, *Nano Energy*, 2021, **83**, 105838.
17. L. Yu, L. Wu, B. McElhenny, S. Song, D. Luo, F. Zhang, Y. Yu, S. Chen and Z. Ren, Ultrafast room-temperature synthesis of porous S-doped Ni/Fe (oxy)hydroxide electrodes for oxygen evolution catalysis in seawater splitting, *Energy Environ. Sci.*, 2020, **13**, 3439-3446
18. R. Jadhav, A. Kumar, J. Lee, T. Yang, S. Na, J. Lee, Y. Luo, X. Liu, Y. Hwang, Y. Liu and H. Lee, Stable complete seawater electrolysis by using interfacial chloride ion blocking layer on catalyst surface, *J. Mater. Chem. A*, 2020, **8**, 24501-24514.
19. M. Ning, F. Zhang, L. Wu, X. Xing, D. Wang, S. Song, Q. Zhou, L. Yu, J. Bao, S. Chen and Z. Ren, Boosting efficient alkaline fresh water and seawater electrolysis via electrochemical reconstruction, *Energy Environ. Sci.*, 2022, **15**, 3945-3957.
20. P. Li, S. Wang, I. A. Samo, X. Zhang, Z. Wang, C. Wang, Y. Li, Y. Du, Y. Zhong, C. Cheng, W. Xu, X. Liu, Y. Kuang, Z. Lu and X. Sun, Common-ion effect triggered highly sustained seawater electrolysis with additional NaCl production, *Research*, 2020, **2020**, 2872141.